Energy Proceedings
Vol 31, 2023
ISSN 2004-2965

Thermo-economic evaluation and optimization of Carnot battery integrating low-grade thermal energy on both charge and discharge processes

Pei Lu[1], Xianglong Luo*, Yingzong Liang, Jianyong Chen, Zhi Yang, Ying Chen

1 School of Material and Energy, Guangdong Provincial Key Laboratory of Functional Soft Matter, Guangdong University of Technology, Guangzhou, China

*Corresponding Author, lxl-dte@gdut.edu.cn

ABSTRACT

This study proposes two configurations of deep integrating low-grade thermal energy during the discharge process of the Carnot battery. The thermodynamic and economic models for pump thermal energy storage, which integrates low-grade thermal energy on charge and discharge processes, are established. The genetic algorithm is used to obtain the optimal operating performance of the proposed Carnot battery, and a comparative analysis is carried out under different design conditions. The results show that the deep thermal integration can significantly improve the operating performance of the Carnot battery during the discharge process. The operating performance of different configurations is significantly affected by the design charging load.

Keywords: Carnot battery, ORC, deep thermal integration, charging loads, integration configurations

NOMENCLATURE

Symbols	
C	Cost ($)
E	Electricity (kWh)
Ex	Exergy (J)
HP	Heat pump
LT	Lifetime (year)
LGTE	Low-grade thermal energy
LCOS	Levelized cost of storage ($/kWh)
ORC	Organic Rankine cycle
PPTD	Pinch point temperature (°C)
PTES	Pump thermal energy storage
r	Discount rate (%)
W	Power (kW)
η	Efficiency (%)
τ	Time (hour)
Superscript and subscript	
an	Annual
com	Compressor
ex	Exergy
exp	Expander
tot	Total
tr	Round-trip

1. INTRODUCTION

The goal of carbon neutrality has driven the development of renewable energy worldwide. Carnot battery is a large-scale power storage technology that has recently emerged to solve the supply imbalance of renewable energy power generation [1]. Among various types of Carnot batteries, pump thermal energy storage (PTES), consisting of the heat pump (HP) and organic Rankine cycle (ORC), has received extensive attention due to its high round-trip efficiency (η_{tr}) and easy thermal integration [2]. Thermal integration-PTES (TI-PTES) can utilize low-grade thermal energy (LGTE) to improve the thermal storage grade and energy conversion efficiency of high-temperature HP [3]. Frate et al. [4] conducted a detailed thermodynamic analysis of the TI-PTES, which showed that the η_{tr} could reach 130% for the LGTE temperature of 110 °C. It is worth noting that the extra heat input is not considered in the

η_{tr}. Therefore, Jockenhofer et al. [5] defined the energetic efficiency, which takes LGTE as energy input in TI-PTES. The results showed that the energetic efficiency (η_{ex}) of TI-PTES can be up to 59%. Considering the trade-off between the operating performance, environmental sustainability, and safety, Eppinger et al. [6] proposed that R1233zd(E) is the most suitable working fluid for TI-PTES. Hu et al. [7] analyzed the thermo-economic performance of TI-PTES under four different operating scenarios. The results showed that geothermal water as the heat source for TI-PTES is the most attractive, with a minimum Levelized cost of storage ($LCOS$) of 0.23 \$/kWh. Previous studies have demonstrated the advantage and feasibility of integrating LGTE in the charging process of HP for the TI-PTES. However, the study on integrating LGTE during the discharge process of ORC is still blank. Since the timing of the storage-release process of TI-PTES is not consistent, the utilization of LGTE is discontinuous, which will cause damage to environmental sustainability. However, it is foreseeable that thermally integrated ORC will boost net power output while increasing costs. Therefore, strategies for thermal integration in ORC are worth investigating.

In this study, we propose two configurations to integrate LGTE during the discharge process of TI-PTES, which are named deep thermally integrated PTES (DTI-PTES). Taking the maximum η_{tr} as the optimization goal and considering the exergy and economic performance, the comparison with TI-PTES under different design boundary conditions is carried out to verify the advantage of the proposed DTI-PTES.

2. PROBLEM DESCRIPTION

This study proposes two integration configurations for integrating LGTE in ORC. In Configuration 1 (C1), the LGTE is integrated into the preheating region of the evaporation process, which needs to add an evaporator in DTI-PTES. Configuration 2 (C2) of DTI-PTES adopts the way of multi-pressure operation to recover the heat of the LGTE and heat storage medium, respectively, which needs to add a pump, an expander, and an evaporator. Fig. 1 shows the *T-s* diagram of three Carnot batteries, where the dotted lines represent the discharge process of the TI-PTES and DTI-PTES.

The charging process is the same for the three Carnot batteries in Fig. 1. The HP drives the compressor with the recovered electric energy to transfer the heat of the LGTE to the heat storage medium (A-B → 5-1 → 2-4 → C-D). For TI-PTES, the ORC transfers the heat in the heat storage medium to the expander to output electrical energy (D-C → 9-6 → 6-7). In C1, after preheating by LGTE (A'-B' → 9-10), the working fluid enters the second evaporator to recover the heat storage load (D-C → 10-6 → 6-7). However, the heat load recovery of the LGTE and the thermal storage medium is separate in C2 (A'-B' → 10-15 → 15-16, D-C → 9-6 → 6-7).

It is evident that the difference between C1 and C2 of DTI-PTES lies in the performance gain of the integrated LGTE. In C1, since the two evaporators that recover the heat storage medium and LGTE are connected in series, the heat storage load mainly limits the mass flow rate of DTI-PTES. Therefore, the heat recovery of LGTE may be insufficient, but C1 will have an advantage in investment cost. In C2, three additional components are required, but more heat load in the LGTE can be recovered, significantly enhancing the ORC's discharge capacity.

3. MATHEMATICAL MODEL

Prior to the modeling, a few assumptions are adopted: (1) The heat loss and pressure drop of each component are neglected. (2) The entire system is operated under steady-state. (3) The working fluid at the outlet of the heat exchanger is saturated vapor. (4)

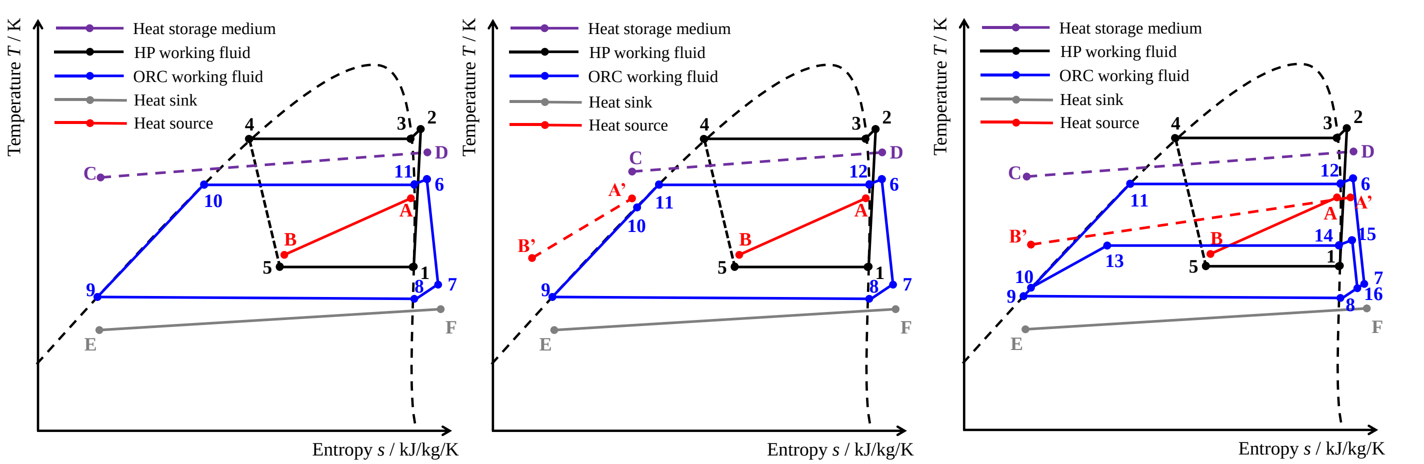

(a) (b) (c)

Fig. 1 *T-s* diagram of Carnot batteries: (a) TI-PTES, (b) Configuration 1 of DTI-PTES, (b) Configuration 2 of DTI PTES.

The isentropic efficiencies of the pump, compressor, and turbine are considered constant. (5) The heat loss of the thermal storage process is not considered.

The η_{tr} is a standard criterion for evaluating the power-to-power efficiency of the Carnot battery.

$$\eta_{\mathrm{tr}} = (W_{\mathrm{exp}} \times \tau_{\mathrm{discharge}})/(W_{\mathrm{com}} \times \tau_{\mathrm{charge}}) \quad (1)$$

In addition, to evaluate the energy conversion of the entire system considering the LGTE input, η_{ex} is also one of the critical indicators of the Carnot battery.

$$\eta_{\mathrm{ex}} = Ex_{\mathrm{ORC}}/(Ex_{\mathrm{HP}} + Ex_{\mathrm{LGTE}}) \quad (2)$$

Besides η_{tr} and η_{ex}, economic performance is also a key criterion for evaluating the application potential of the Carnot battery. Since the $LCOS$ is a widely used metric to compare different storage technologies, $LCOS$ is chosen to evaluate the TI-PTE and DTI-PTES. The economic model is modeled regarding Ref. [8].

$$LCOS = \frac{C_{tot} + \sum_{i=1}^{LT} C_{an}/(1+r)^i}{\sum_{i=1}^{LT} E_{\mathrm{exp}}/(1+r)^i} \quad (3)$$

In this study, aiming at maximizing η_{tr}, a genetic algorithm is used to optimize the of TI-PTES and DTI-PTES. The thermodynamic and economic models for three Carnot batteries are constructed, the energetic, exergetic, and economic performances of the TI-PTES and DTI-PTES are calculated and analyzed.

4. RESULTS AND DISCUSSION

This subsection analyzes the differences in the thermodynamic and economic performance of the TI-PTES and two configurations of DTI-PTES. We set up two design scenarios with different charging capacities for the above comparison. In addition, R1233zd(E) is selected as the working fluid in this study according to the result of Ref. [6]. The primary parameter settings of the three Carnot batteries are shown in Table 1.

Taking a compressor load of 1 MW as the first design scenario, Fig. 2 shows the optimization results for three Carnot batteries. It can be seen that the thermodynamic and economic properties of DTI-PTES are stronger than TI-PTES, which verifies the superiority of the proposed system. Among them, C2 of DTI-PTES has the best performance, with η_{tr} of 89.76% and η_{ex} of 51.45%. The thermal storage load does not limit the mass flow rate of working fluid in C2, and the working fluid can absorb more heat from LGTE for power generation. So even with higher investment costs, C2 of DTI-PTES still has the lowest $LCOS$, which is as low as 0.07 \$/kWh. In addition, the mass flow rate in the ORC system in C1 is much smaller than that in the HP system due to two heat transfer losses in transferring energy from the HP to the ORC. Therefore, the working fluid in ORC of C1 cannot perfectly absorb the energy brought by LGTE during the preheating process, and there is more exergy destruction. Therefore, the operating performance of C1 is worse than that of C2 of DT-PTES while still better than TI-PTES. Overall, the η_{tr} of C2 is 32.11% higher than that of C1 and 75.84% higher than that of TI-PTES. Compared with C1 of DTI-PTES and TI-PTES, the η_{ex} of C2 is improved by 30.22% and 69.66%, respectively.

Table 1 Main parameter assumptions for Carnot Batteries.

Parameter item	Value
Working fluid	R1233zd(E)
Heat storage medium	Water
Heat source medium	Geothermal water
Heat sink medium	Cooling water
Isentropic efficiency of the pump (%)	75
Isentropic efficiency of the expander (%)	75
Isentropic efficiency of the compressor (%)	75
Heat storage efficiency (%)	100
Heat source mass flowrate (kg/s)	100,1000
Heat source inlet temperature (°C)	60
Heat sink inlet temperature (°C)	10
Heat sink temperature rise (°C)	10
Superheat/subcooling degree (°C)	0
Storage temperature lift (°C)	≥10
Heat storage pressure (kPa)	101.325
Minimum pressure of the exchanger (kPa)	101.325
Minimum *PPTD* of the exchanger (°C)	2
Ambient temperature (°C)	5
Storage duration (hour)	8
Electricity price (\$/kWh)	0.05
Water price (\$/kg)	0.0016
Discount rate (%)	5
Lifetime (year)	25

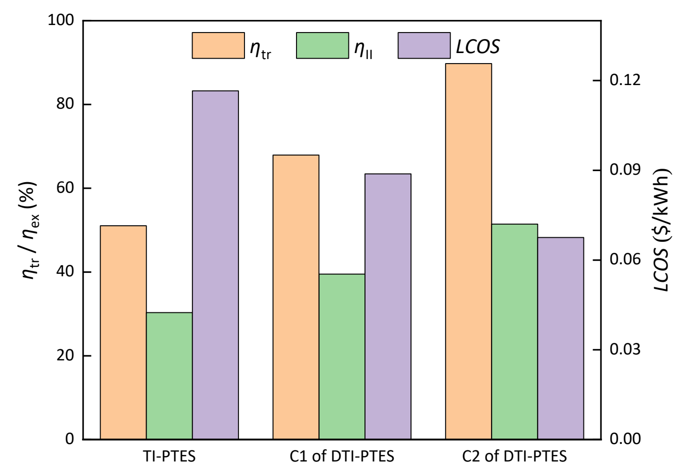

Fig. 2 The optimization results of the TI-PTES and DTI-PTES under the design scenario with a 1 MW compressor load.

The optimization results changed in the second design scenario with a 10 MW charge load, as shown in Fig. 3. Likewise, DTI-PTES performs better than TI-PTES in thermodynamic and economic performance. However, the performance of C1 is better than that of C2 of DTI-PTES, which performs a η_{tr} of 60.56% and η_{ex} of 34.71%. The results are that the working fluid in the ORC of C1 can more effectively utilize the thermal energy of LGTE in the preheating section due to the enormous mass flow rate. Therefore, the heat matching of working fluid with LGTE and heat storage medium has an excellent performance in C1 of DTI-PTES. However, the exergy destruction in the two evaporators in C2 is amplified because of the larger mass flow rate. C1 of DTI-PTES has a lower $LCOS$ of 0.20$/kWh due to the addition of only one set of heat exchangers. It can be seen that the operating performance of different configurations of DTI-PTES is significantly affected by the design charging load. The results can provide a reference for designers and investors.

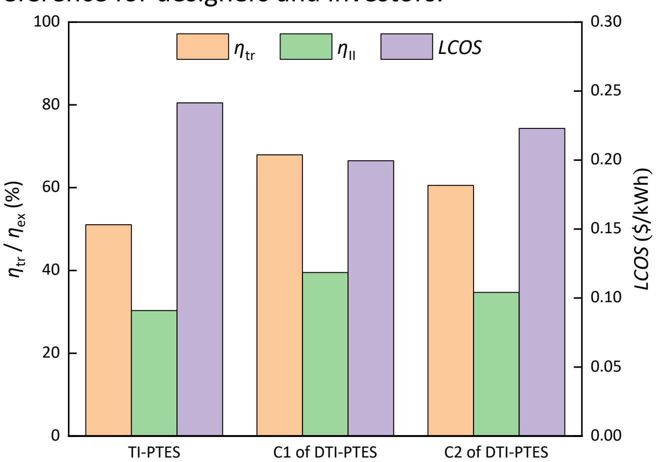

Fig. 3 The optimization results of the TI-PTES and DTI-PTES under the design scenario with a 10 MW compressor load.

5. CONCLUSION

This study proposes two DTI-PTES configurations that deeply integrate the LGTE during the discharge process. Two design scenarios with different charging capacities are set to compare the energetic, exergetic, and economic performances of the TI-PTES and DTI-PTES. The thermodynamic performance of three Carnot Batteries was optimized by genetic algorithm. Following conclusions were drawn.

DTI-PTES outperforms TI-PTES in thermodynamic and economic performance in all design scenarios. When the charging load is 1 MW, C2 of DTI-PTES with η_{tr} of 89.76%, η_{ex} of 51.45%, and $LCOS$ of 0.07 $/kWh has the best performance among the three Carnot Batteries. The heat storage load does not limit the mass flow rate of working fluid in C2, which makes the working fluid absorb more heat from LGTE for power generation. In contrast, the mass flow rate of C1 is limited from the heat storage load.

For the charging load of 10 MW, the best performing Carnot battery is C2 of DTI-PTES, with η_{tr} of 60.56%, η_{ex} of 34.71%, and $LCOS$ of 0.20 $/kWh. The working fluid of C1 can better match the LGTE and heat storage medium during the evaporating process at higher mass flow rates. In comparison, the exergy loss in two evaporators of C2 of DTI-PTES is amplified under the same conditions. The results can provide a reference for designers and investors.

It is noticed that the operating performance of DTI-PTES in different modes is more sensitive to the charging loads. Therefore, an exploration of the topology of DTI-PTES under different boundary conditions and a multi-objective optimization study between its thermal and economic performance will be implemented in our future research.

ACKNOWLEDGMENT

The authors gratefully acknowledge the financial support from the National Natural Science Foundation of China (Grant No. 51876043) and Guangdong Special Support Program (Grant No. 2017TX04N371).

REFERENCES

[1] Francesco Frate Guido, Ferrari Lorenzo, Desideri Umberto. Rankine Carnot batteries with the integration of thermal energy sources: A review. Energies 2020;13:4766.

[2] Dumont Olivier, Francesco Frate Guido, Pillai Aditya, Lecompte Steven, De Paepe Michael, Lemort Vincent. Carnot battery technology: A state-of-the-art review. J Energy Storage 2020;32:101756.

[3] Steinmann W.D. The CHEST (Compressed heat energy storage) concept for facility scale thermo mechanical energy storage. Energy 2014;69:543-552.

[4] Francesco Frate Guido, Antonelli Marco, Desideri Umberto. A novel pumped thermal electricity storage (PTES) system with thermal integration. Appl Therm Eng 2017;121:1051-1058.

[5] Jockenhöfer Henning, Steinmann Wolf-Dieter, Bauer Dan. Detailed numerical investigation of a pumped thermal energy storage with low temperature heat integration. Energy 2018;145:665-676.

[6] Eppinger Bernd, Zigan Lars, Karl Jürgen, Will Stefan. Pumped thermal energy storage with heat pump-ORC-

systems: Comparison of latent and sensible thermal storages for various fluids. Appl Energy 2020;280:115940.
[7] Hu Shuozhuo, Yang Zhen, Li Jian, Duan Yuanyuan. Thermo-economic analysis of the pumped thermal energy storage with thermal integration in different application scenarios. Energy Convers Manage 2021;236:114072.
[8] Fan Ruoxuan, Xi Huan. Energy, exergy, economic (3E) analysis, optimization and comparison of different Carnot battery systems for energy storage. Energy Convers Manage 2021;51:104453.